Hindawi
International Journal of Corrosion
Volume 2019, Article ID 2123547, 7 pages
https://doi.org/10.1155/2019/2123547

Research Article

Effects of Chlorides on Corrosion of Simulated Reinforced Blended Cement Mortars

Jackson Muthengia Wachira

Department of Physical Sciences, University of Embu, Embu, Kenya

Correspondence should be addressed to Jackson Muthengia Wachira; wachira.jackson@embuni.ac.ke

Received 8 December 2018; Revised 2 March 2019; Accepted 17 March 2019; Published 27 March 2019

Academic Editor: Ramana M. Pidaparti

Cementitious materials are subject to degradation when subjected to corrosive chloride media. This paper reports the experimental results on corrosion studies conducted on a potential cementitious material, PCDC, made from a blend of 55 % Ordinary Portland Cement (OPC), Dried Calcium Carbide Residue (DCCR), and an incineration mix of Rice Husks (RH), Spent Beaching Earth (SBE), and Ground Reject Bricks (BB). The experiments were run along 100 % OPC. Different w/c were used. Corrosion current densities using linear polarisation resistance (LPR) and corrosion potentials measurements versus saturated calomel electrode were used for the determination of corrosion rates and potentials, respectively, for simulated reinforcement at different depths of cover in the cement mortars. The results showed that PCDC exhibited higher corrosion current densities over all depths of covers and early attainment of active corrosion than the control cements. In conclusion, PCDC and OPC can be used in a similar corrosive media during construction.

1. Introduction

Reinforcing metal in concrete is usually protected by a layer of the iron oxide/iron hydroxide and the high concrete pH[1–3]. The protective layer is a film of the gamma ferric oxides (γ-Fe_2O_3), iron oxide hydroxide [FeO(OH)] and magnetite (Fe_3O_4) which prevent Fe^{2+} from entering into the solution as well as oxygen from diffusing to the steel surface[4]. The layer has also been found to be rich in lime with inclusions of C-S-H gel [5, 6]. The high electric resistivity of concrete is also another aspect that helps in corrosion resistance of the rebar. This acts by reducing the flow of current between the cathodic and anodic sites of the rebar.

When reinforced concrete comes into contact with chlorides at levels beyond certain critical conditions, pitting corrosion ensues. These levels are generally defined in terms of Cl^-/OH^- threshold of the mortar or concrete. This has generally been agreed to be about 0.6, although some authors have observed different values [1, 7]. In an aerated chloride solution, at the critical Cl^-/OH^- threshold, the chlorides cause dissolution of the protective layer of the oxides of iron and thus dissolution of the metal in the pit [1, 6, 8]. This creates charge difference, as a result of excess positive metal ions, forcing Cl^- ions to rapidly migrate into the pit giving rise to metal chloride. The reactions involved are given in (1)–(3). They represent that the anodic reaction because corrosion is an electrochemical reaction [9]:

$$Fe(OH)_2 + 2Cl^- \longrightarrow FeCl_2 + 2OH^- \tag{1}$$

$$Fe(OH)_3 + 3Cl^- \longrightarrow FeCl_3 + 3OH^- \tag{2}$$

$$Fe_2O_3 + 6Cl^- + 3H_2O \longrightarrow 2FeCl_3 + 6OH^- \tag{3}$$

The resultant metal chloride undergoes hydrolysis, as shown in (4), consequently causing a build-up of the hydrogen and chloride ions that stimulate dissolution of the metal [10].

$$FeCl_n + nH_2O \longrightarrow Fe(OH)_n + nHCl \tag{4}$$

where n = 2 or 3 depending on the oxidation state of Fe.

Since there is limited dissolution of oxygen in the pit solution, the cathodic reduction of dissolved oxygen on the metal surface adjacent to the pit sustains the pit growth. The cathodic site, the metal surface, is very large compared to the pit size, and this makes the pit grow at a fast and an ever increasing rate [11].

The cathodic reactions involved depend on the pH and potential of the rebar. Hydrogen evolution and oxygen reduction are mainly involved [9]. Hydrogen evolution does not take place unless in condition of cathodic protection or circumstances with low pH and at conditions where the rebar has potentials more active than $E^{\theta}_{H^+/H_2}$(SHE). Ordinary corrosion of rebar under chloride initiation involves oxygen reduction as shown by the following [12];

$$O_2 + 4H_2O + 4e^- \longrightarrow 4OH^- \quad (5)$$

The mechanical performance of a potential cementitious material, PCDC, made from a blend of 55 % Ordinary Portland Cement (OPC), Dried Calcium Carbide Residue (DCCR), and an incineration mix of Rice Husks (RH), Spent Beaching Earth (SBE), and Ground Reject Bricks (BB) has been reported in previous studies. However, the durability of PCDC in corrosive media has not been conducted. The present study therefore investigated the corrosion rates and potentials of PCDC vis-a-vis commercial OPC in simulated reinforcement at different depths of cover using the test cement mortars

2. Materials and Methods

2.1. Materials. 10 mm by 80 mm mild steel rods, whose chemical composition is given in Table 1 (as analysed by the Bureau Veritas Consumer Products Services UK LTD) were cut and smoothened on the edges with a smooth file. The rods were polished with emery papers 80-600 grit in succession. The resulting metal rods were washed with distilled water, rinsed with acetone, and blow dried. They were stored in a desiccator that used silica as desiccant.

Table 2 shows the various compositions of materials used in this study.

2.2. Methods

2.2.1. Preparation of Simulated Reinforced Mortars. 3:1 sand to binder (100 % OPC or PCDC) ratio was used in preparation of the mortar. In the initial stages, it was presumed that mortar with 0.4, 0.5 and 0.6 w/c ratio would be prepared. It was however noted that the amount of water added to correspond with the above w/c ratios could not make consistent pastes. This was because the sand was oven dried. Laboratory tests revealed the oven dried sand would require an amount of water corresponding to 0.077 percent by weight of sand to correlate with non-oven dried sand. A 0.8 w/c ratio mortar proved to be the best workable mix with the three cement categories. A lower w/c ratio of 0.73 was also used but the paste was observed to have a poor workability. A higher w/c ratio of 0.85 was also prepared. A corrected w/c ratio after taking into account the oven dried sand was found to be 0.5, 0.57 and 0.62 for 0.73, 0.8, and 0.85, respectively. To avoid confusion, the later w/c ratios have been used in this paper.

Six 30 mm by 100 mm by 100 mm high density PVC were machine cut. Six 10 mm hole were drilled through the PVC blocks. From one edge of the blocks, two holes were drilled at 20 and two more at 15 mm from the other edge. A hole was drilled through on the remaining edges at 10 mm from the edge. Holes with dimensions and distances from the edges, similar to the PVC block, were made on a 0.5 mm by 100mm by 100 mm polythene sheet. The PVC block was lightly spot-oiled with an oil-dump tissue paper. The polythene sheet was placed on the PVC block and the holes on either matched. The PVC block plus the polythene sheet were placed at the bottom of a cube mould. The polished mild steel rods were carefully and gently pushed into the PVC block holes. Two such cube moulds were placed on a vibrating bench. Mortar was carefully shovelled into the cubes and compaction done for about 30 seconds. The mortar was levelled using a trowel and vibration continued for about 10 seconds. Final levelling was done. The resultant mortar was cured for 24 hours (in case of 0.73 and 0.8 w/c ratio) and 48 hours (in case of 0.85 w/c ratio) after which they were demoulded.

On the second day after preparation of individual mortar cubes, 6 mm nichrome wires with 5 mm heat shrunk tubings were spot welded at about 8 mm from the top side of the protruding rebar. After the sixth day of preparing all the cubes, steel reinforcement protector 841, obtained from Flexcrete Technologies Limited (UK), was applied to the mortars with embedded steel rods. This was done by first gritting the exposed surface of the rods with emery paper grade 80 and then deoiling the protruding rebar ends with acetone soaked cloth. Steel reinforcement protector was prepared by mixing 3: 1 by volume of cementitious powder to polymer dispersion provided and thoroughly mixing it with the help of a provided wooden stick to a brushable paste. The resultant paste was thinly applied to about 1 mm with a 25 mm pure bristles brush on the exposed ends of the rebars. The steel reinforcement protector 841 paste was similarly applied on to the mortar cube to the face with the exposed rebar surface. The first coat was allowed to cure for about 45 minutes before application of a similar second coat on top of the first one. After an additional 45 minutes, any voids were brushed with the steel reinforcement protector 841 paste. The mortar cubes were allowed to cure overnight. The mortar cubes were cured for an additional 21 days in saturated calcium hydroxide solution. After the 28th day of curing, 2-metre insulated copper cables were connected to the nichrome wire spot welded to the embedded steel rods with the help of joint clips. The open ends of the clips were sealed with silicon based sealant Dow Corning 732. The insulated copper cables were labelled with a seven code identity as shown in Table 3. All cubes were subjected to one-week alternate wet-dry tank for a period of six months. The wet alternate week involved complete immersion of the mortar cubes in 3.5 percent sodium chloride solution.

2.2.2. Corrosion Current Densities and Potential Measurements. Corrosion potentials, E_{corr}, were measured using saturated calomel electrode (SCE) as reference electrode with a high impedance voltmeter. Linear polarisation resistance (LPR) was done using a potentiostat using SCE and graphite rod as reference and counter electrode, respectively. The LPR

Table 1: Chemical composition of mild steel.

Element	% w/w	Method of Analysis
C	0.18	Combustion Analysis
Si	0.23	ICPOES
Mn	0.77	ICPOES
P	0.016	ICPOES
S	0.011	Combustion Analysis
Cr	0.03	ICPOES
Mo	<0.02	ICPOES
Ni	0.04	ICPOES
Al	0.032	ICPOES
Co	<0.005	ICPOES
Cu	0.09	ICPOES
Nb	<0.005	ICPOES
Pb	<0.02	ICPOES
Sn	<0.02	ICPOES
Ti	0.005	ICPOES
V	<0.02	ICPOES
W	<0.02	ICPOES
Fe	Balance	

ICPOES: Inductively Coupled Plasma Optical Emission Spectroscopy.

Table 2: Compositions of various materials.

Material	Description
OPC	Commercial Ordinary Portland Cement (42.5 N/mm)
PPC	Commercial Portland Pozzolana Cement or Blended Cement (32.5 N/mm)
Test Ash	A blend of DALS and a calcined mix of RH, SBE, ground BB
PCDC	A blend of 55 % OPC and 45 % Test Ash

Table 3: Description of the insulated copper cables.

Material	Composition	Water/cement ratio (w/c)	Depth of rebar (mm)
OP12GL	OPC	0.73	20
OP12BL	OPC	0.73	15
OP12YL	OPC	0.73	10
OP29GL	OPC	0.85	20
OP29BL	OPC	0.85	15
OP29YL	OPC	0.85	10
OP31GL	OPC	0.83	20
OP31BL	OPC	0.83	15
OP31YL	OPC	0.83	10
PC12GL	PCDC	0.73	20
PC12BL	PCDC	0.73	15
PC12YL	PCDC	0.73	10
PC29GL	PCDC	0.85	20
PC29BL	PCDC	0.85	15
PC29YL	PCDC	0.85	10
PC31GL	PCDC	0.83	20
PC31BL	PCDC	0.83	15
PC31YL	PCDC	0.83	10

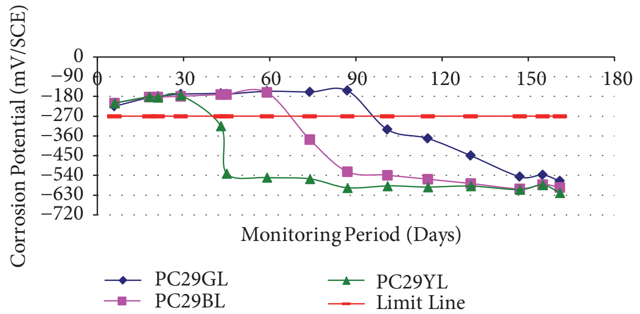

FIGURE 1: Corrosion potential versus time for PCDC at w/c of 0.85.

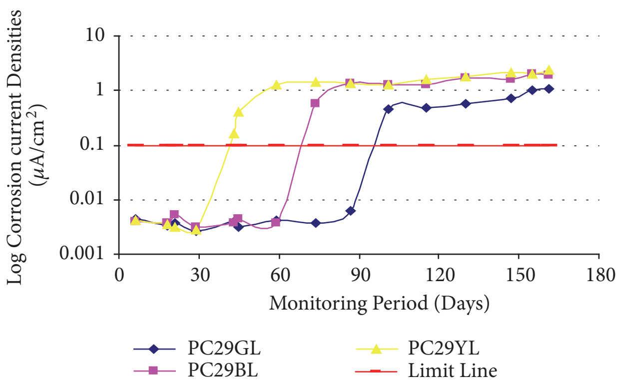

FIGURE 2: Log corrosion current densities versus time for PCDC at w/c 0.85.

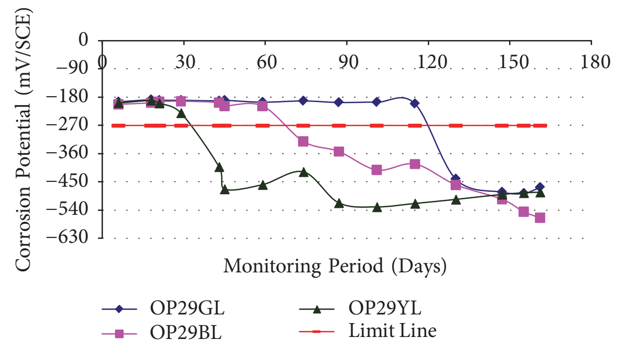

FIGURE 3: Corrosion potential versus time for OPC at w/c of 0.85.

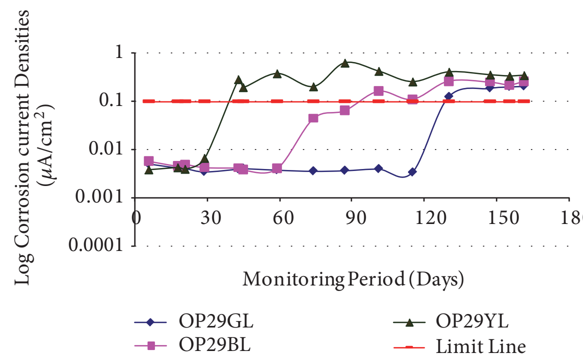

FIGURE 4: Log corrosion current densities versus time for OPC at w/c 0.85.

and potential measurements were done for a total of 12 wet-dry cycles which coincided with 168 days. E_{corr} and LPR measurements were done during the wet seasons.

In LPR measurements, the potential was manually shifted from E_{corr} to ± 20 mV in intervals of about 5-8 mV this is because, at this range, no significant noise was expected in the instrument. Corrosion current readings were taken after stabilisation which took about 45–60 seconds. A graph of overpotentials, η, versus corrosion current was plotted and its gradient, R_P, calculated. Corrosion current density, i_{corr}, was determined as per

$$i_{corr} = \frac{52}{(S_A * R_P)} \tag{6}$$

where S_A is the specific surface area of the rebar, approximated from $(\pi Dh + \pi r^2)$ in which cases D, h, and r represent diameter, height, and radius of the rebar, respectively. The height, h, taken was for the length of the rebar embedded in the mortar cube. 52 mV/decade was taken as the Tafel constant in all the cases.

3. Results and Discussion

3.1. Corrosion Current Densities, i_{corr}, and Corrosion Potentials. Figures 1–12 represent the corrosion current densities, i_{corr}, and corrosion potentials, E_{corr} of the respective simulated reinforced cement mortar at the defined w/c versus curing period. Working electrodes that had attained an i_{corr} value of greater than or equal to 0.1 μA/cm^2 were considered to have attained active corrosion [13]. Similarly, rebars that had attained E_{corr} more active than -270 mV (Vs SCE) were taken to have attained active corrosion. The limit lines in Figures 1–12 represent the limits above or below these lines (i_{corr} and E_{corr}, respectively)

The results showed that the depth of cover was an important parameter because the rebars at the shallow depth of cover attained active corrosion earlier than their counterparts at greater depths of cover. This is because the chlorides have lower distance to diffuse and initiate pitting type of corrosion. Hence there is a lower resistivity due to the reduced concrete cover at lower depths of cover.

PCDC's rebars exhibited earlier attainment of active corrosion compared to OPCs. The inclusion of lime in cements is known to increase porosity [14, 15]. PCDC had a significant proportion of lime added in form of DALS. This may have served to increase porosity of the cement mortar at the initial stages of curing. Upon attainment of active corrosion by the 0.85 (w/c) cements, PCDC's rebar registered higher i_{corr} than corresponding OPC's rebar. Some workers have attributed the higher corrosion rates by substituted cements' rebars to the lowering of pore pH by the pozzolanic reaction [16]. In previous related studies, chloride binding ability and its influence on the rate of corrosion on OPC and its blended cements of GGBS, PFA, and SF showed that despite higher chloride binding ability of blended cements and higher chloride concentration in OPC's pore solution, the corrosion

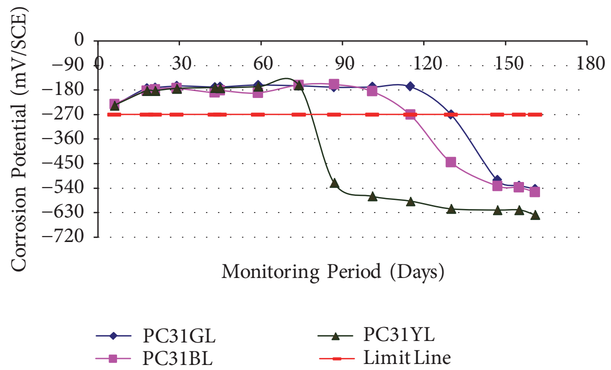

FIGURE 5: Corrosion potential versus time for PCDC at w/c of 0.80.

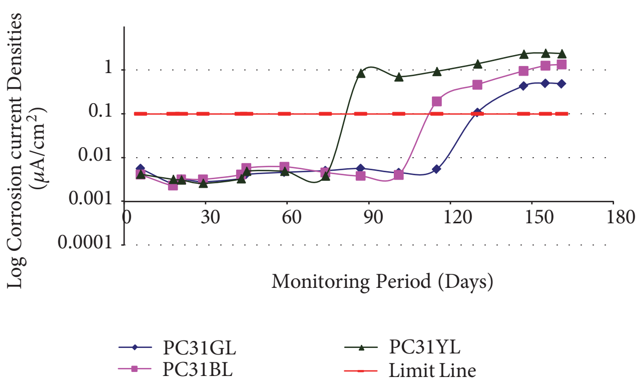

FIGURE 6: Log corrosion current densities versus time for PCDC at w/c 0.80.

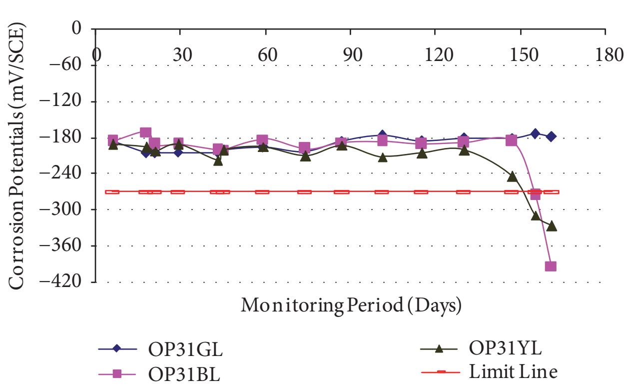

FIGURE 7: Corrosion potential versus time for OPC at w/c of 0.80.

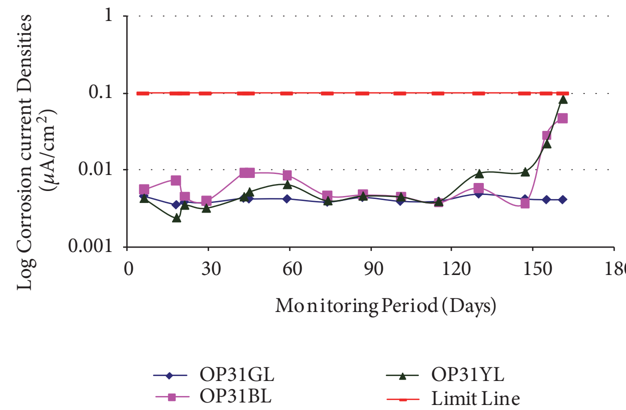

FIGURE 8: Log corrosion current densities versus time for OPC at w/c 0.80.

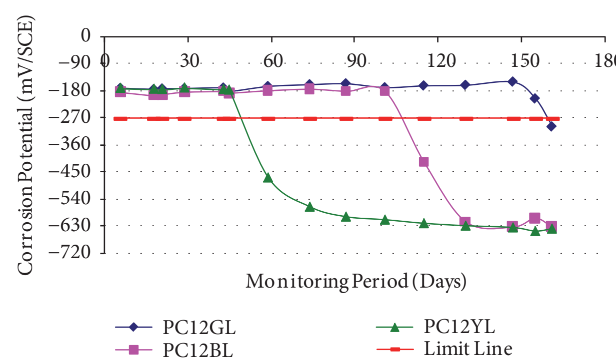

FIGURE 9: Corrosion potential versus time for PCDC at w/c 0.73.

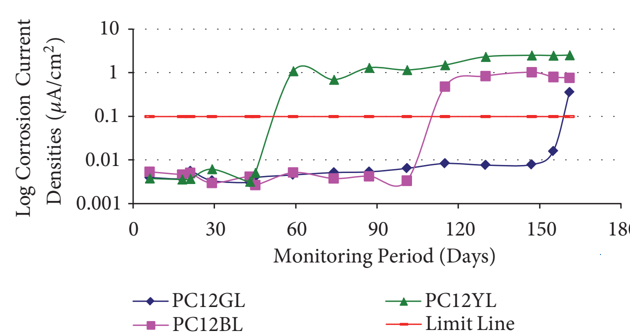

FIGURE 10: Log corrosion current densities versus time for PCDC at w/c 0.73.

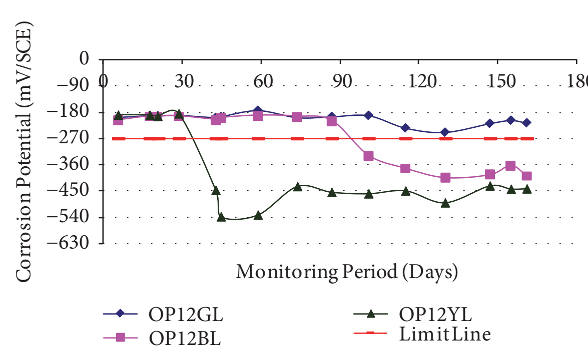

FIGURE 11: Corrosion potential versus time for OPC at w/c of 0.73.

rates of the rebars in OPC were lower than the blended cements [17]. This can be attributed to the higher corrosion rates to a lower OH^- in the blended cements pore solution. The decline in pore solution OH^- to both dilution factor (lower OPC content) and chemical activity of the pozzolana materials may have affected the PCDC cements and hence its rebars exhibited higher corrosion rates compared to OPCs.

At a lower water to cement ratio, for example, 0.8, there was delay in rebar corrosion initiation time for both cements compared to the w/c of 0.85. This was due to reduced porosity and hence diffusivity of the chlorides and

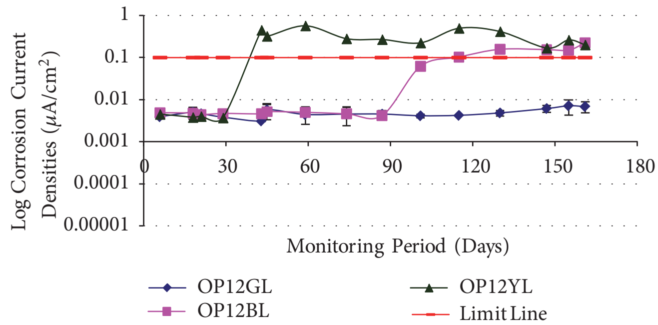

Figure 12: Log corrosion current densities versus time for OPC at w/c 0.73.

oxygen. Lower w/c is a well-known factor that reduces the permeability of concrete and hence diffusivity of aggressive agents [18].

It was observed that increase in w/c ratio increased the penetration of chlorides. This can be attributed to the fact that there is a decrease in porosity within the lime-cement based mortar as the w/c ratio reduced [19]. When lime is added to the PCDC as DALS, the effect of reduced porosity due to lower w/c ratio must have been experienced in the PCDC. This may have resulted in the increase in initiation time for the rebars corrosion compared to the higher w/c ratio.

Increasing w/c ratio is also known to increase the oxygen diffusivity into the mortar cubes [20, 21]. Oxygen diffusion is an important factor that plays a major role in the corrosion of the rebar. This is because oxygen is the main cathodic reaction in rebar corrosion. At higher oxygen diffusivity, the cathodic reaction is high, so is the anodic (rebar corrosion) and therefore the corrosion rate. Oxygen dissolved in the pore solution is important in as far as maintaining the passivity (iron oxides films on the rebar). This prevents the rebar from corrosion. Sustenance of corrosion (pitting type in this case) is dependent on the sufficient supply of oxygen through the cathodic reaction on the passive film [21].

OPC rebars at 15 and 20 mm depth of cover and w/c ratio of 0.73 did not attain active corrosion as indicated by the corrosion current densities. Observations from the corrosion potentials (versus SCE) and visual examination of rebars, after dismantling the cubes, indicated that there was active corrosion of the rebars at the depth of 10 mm and a very slight corrosion on rebars at 15 mm. Probably the time interval of dismantling of the mortar cube and last measurement of the rebars may have attained appreciable corrosion for the rebars at 15 mm depth of cover.

Despite poor compaction in both mortars at the w/c of 0.73, PCDC exhibited delayed initiation of active corrosion at the 10 mm depth of cover compared to OPC. Thus delayed active corrosion was expected for the rebars at the 15 and 20 mm depth of cover but the opposite happened: PCDC's rebar attained active corrosion while OPC's rebars did not. This could perhaps have resulted from voids around the rebars due to poor compaction. This would thus have availed a high chloride ingress at the rebar that would have been sufficient enough to initiate corrosion and hence the observed behaviour. A more insight study on the porosity and hence permeability would thus be required to provide information on the same for such low w/c ratio of PCDC.

PCDC's rebars were observed to have higher corrosion rates and earlier attainment of active corrosion compared to OPCs. The reduction of the pore pH due to pozzolanic reaction, even at low chloride concentration, increases iron solubility due to formation of stable chlorocomplex (of $Fe^{2+/3+}$) corrosion products (mainly green rust). These products are easily oxidised and precipitated as β–FeOOH (Akagenite) by diffused oxygen thereby releasing the Cl^-. This regenerates the Cl^- that replenishes the cycle which in essence destabilises the passive layer. Decrease in Cl^-/OH^- ratio is a contributing factor to early corrosion initiation phenomenon in blended cements [22]. Perhaps this could be attributed to its high level of substitution.

4. Conclusion

It was generally noted that PCDC's rebars experienced early active corrosion and higher corrosion rates compared to corresponding OPC's rebars.

Data Availability

The data used in this article will be provided upon request.

Conflicts of Interest

The author declares no conflicts of interest in this paper.

Acknowledgments

The author wish to acknowledge the assistance accorded to this work by Kenyatta University and The University of Manchester. This work was financially supported by Kenyatta University.

References

[1] C. Alonso, C. Andrade, M. Castellote, and P. Castro, "Chloride threshold values to depassivate reinforcing bars embedded in a standardized OPC mortar," *Cement and Concrete Research*, vol. 30, no. 7, pp. 1047–1055, 2000.

[2] N. Amin, S. Alam, and S. Gul, "Effect of thermally activated clay on corrosion and chloride resistivity of cement mortar," *Journal of Cleaner Production*, vol. 111, pp. 155–160, 2016.

[3] M. Balonis, *The Influence of Inorganic Chemical Accelerators and Corrosion Inhibitors on the Mineralogy of Hydrated Portland Cement Systems*, Aberdeen University, 2010.

[4] D. M. Bastidas, A. Fernández-Jiménez, A. Palomo, and J. A. González, "A study on the passive state stability of steel embedded in activated fly ash mortars," *Corrosion Science*, vol. 50, no. 4, pp. 1058–1065, 2008.

[5] P. Chindaprasirt and S. Rukzon, "Strength, porosity and corrosion resistance of ternary blend Portland cement, rice husk ash and fly ash mortar," *Construction and Building Materials*, vol. 22, no. 8, pp. 1601–1606, 2008.

[6] S. A. Civjan, J. M. LaFave, J. Trybulski, D. Lovett, J. Lima, and D. W. Pfeifer, "Effectiveness of corrosion inhibiting admixture combinations in structural concrete," *Cement and Concrete Composites*, vol. 27, no. 6, pp. 688–703, 2005.

[7] M. U. Khan, S. Ahmad, and H. J. Al-Gahtani, "Chloride-induced corrosion of steel in concrete: an overview on chloride diffusion and prediction of corrosion initiation time," *International Journal of Corrosion*, vol. 2017, Article ID 5819202, 9 pages, 2017.

[8] C. Monticelli, M. Natali, A. Balbo et al., "Corrosion behavior of steel in alkali-activated fly ash mortars in the light of their microstructural, mechanical and chemical characterization," *Cement and Concrete Research*, vol. 80, pp. 60–68, 2016.

[9] R. R. Hussain and T. Ishida, "Enhanced electro-chemical corrosion model for reinforced concrete under severe coupled action of chloride and temperature," *Construction and Building Materials*, vol. 25, no. 3, pp. 1305–1315, 2011.

[10] K. O. Ampadu and K. Torii, "Chloride ingress and steel corrosion in cement mortars incorporating low-quality fly ashes," *Cement and Concrete Research*, vol. 32, no. 6, pp. 893–901, 2002.

[11] M. Babaee and A. Castel, "Chloride-induced corrosion of reinforcement in low-calcium fly ash-based geopolymer concrete," *Cement and Concrete Research*, vol. 88, pp. 96–107, 2016.

[12] B. Pradhan and B. Bhattacharjee, "Performance evaluation of rebar in chloride contaminated concrete by corrosion rate," *Construction and Building Materials*, vol. 23, no. 6, pp. 2346–2356, 2009.

[13] Ş. Erdoğdu, T. Bremner, and I. Kondratova, "Accelerated testing of plain and epoxy-coated reinforcement in simulated seawater and chloride solutions," *Cement and Concrete Research*, vol. 31, no. 6, pp. 861–867, 2001.

[14] S. Abo-El-Enein, G. El-kady, T. El-Sokkary, and M. Gharieb, "Physico-mechanical properties of composite cement pastes containing silica fume and fly ash," *HBRC Journal*, vol. 11, no. 1, pp. 7–15, 2015.

[15] M. J. Mwiti, T. J. Karanja, and W. J. Muthengia, "Properties of activated blended cement containing high content of calcined clay," *Heliyon*, vol. 4, no. 8, Article ID e00742, 2018.

[16] C. Arya, N. R. Buenfeld, and J. B. Newman, "Factors influencing chloride-binding in concrete," *Cement and Concrete Research*, vol. 20, no. 2, pp. 291–300, 1990.

[17] C. Arya and Y. Xu, "Effect of cement type on chloride binding and corrosion of steel in concrete," *Cement and Concrete Research*, vol. 25, no. 4, pp. 893–902, 1995.

[18] H. Yiğiter, H. Yazıcı, and S. Aydın, "Effects of cement type, water/cement ratio and cement content on sea water resistance of concrete," *Building and Environment*, vol. 42, no. 4, pp. 1770–1776, 2007.

[19] M. Mosquera, B. Silva, B. Prieto, and E. Ruiz-Herrera, "Addition of cement to lime-based mortars: Effect on pore structure and vapor transport," *Cement and Concrete Research*, vol. 36, no. 9, pp. 1635–1642, 2006.

[20] K. Kobayashi and K. Shuttoh, "Oxygen diffusivity of various cementitious materials," *Cement and Concrete Research*, vol. 21, no. 2-3, pp. 273–284, 1991.

[21] R. R. Hussain and T. Ishida, "Influence of connectivity of concrete pores and associated diffusion of oxygen on corrosion of steel under high humidity," *Construction and Building Materials*, vol. 24, no. 6, pp. 1014–1019, 2010.

[22] A. M. Oliveira and O. Cascudo, "Effect of mineral additions incorporated in concrete on thermodynamic and kinetic parameters of chloride-induced reinforcement corrosion," *Construction and Building Materials*, vol. 192, pp. 467–477, 2018.